Hydraulic fracture at dam-foundation joint

F. Barpi[1] and S. Valente[2]

Department of Structural and Geotechnical Engineering, Politecnico di Torino,
Corso Duca degli Abruzzi 24, 10129 Torino, Italy.
[1]Tel: +39 11 5644886, Fax: +39 11 5644899, e-mail: *fabrizio.barpi@polito.it*
[2]Tel: +39 11 5644853, Fax: +39 11 5644899, e-mail: *silvio.valente@polito.it*

ABSTRACT. *When fracture occurs in a concrete dam, the crack mouth is typically exposed to water. Very often this phenomenon occurs at the dam-foundation joint and is driven also by the fluid pressure inside the crack. Since the joint is the weakest point in the structure, this evolutionary process determines the load bearing capacity of the dam. In this paper the cracked joint is analysed through the model proposed by Cocchetti, Maier and Shen [1] which takes into account the coupled degradation of normal and tangential strength. The water pressure inside the crack, which reduces fracture energy and increases the driving forces, is analysed through the model proposed by Reich, Brühwiler, Slowik and Saouma [2]. Some numerical results are presented which refer to the benchmark problem proposed in 1999 by the International Commission On Large Dams [3]. In concrete dams, cracks are present and may be of considerable dimensions since the beginning of dam life. When fictitious process zone is completely developed and the water penetrates inside the crack, a small cycle in water level is enough to make locally a complete unloading and reloading cycle.*

INTRODUCTION

When cracking occurs in a concrete dam the crack mouth is typically exposed to water. Very often this phenomenon occurs at the dam-foundation joint and is driven also by the fluid pressure inside the crack. Since the joint is the weakest point in the structure, this evolutionary process determines the load bearing capacity of the dam. In this paper the cracked joint is analysed through the model proposed by Cocchetti, Maier and Shen ([1], shortened CMS) which takes into account the coupled degradation of normal and tangential strength at the dam/foundation interface. The water pressure inside the crack, which reduces fracture energy and increases the driving forces, is analysed through the model proposed in [2]. The crack opening displacement induces two consequences: (a) concrete permeability increases, and (b) water pressure increases. Each one of these two phenomena drives the other. Some results are presented which refer to the benchmark problem proposed in 1999 by the International Commission On Large Dams [3]. Similar water/fracture interaction phenomena are observed in the analysis of retaining walls and rock slope stability.

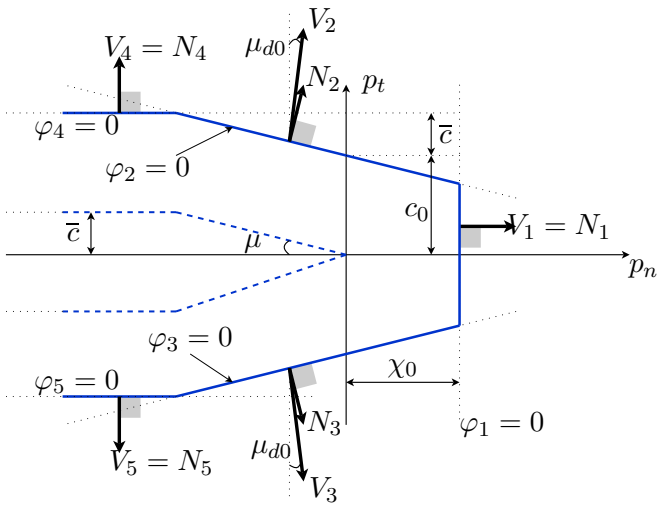

Figure 1. Piecewise linear model.

JOINT MODELS

A joint is a locus of possible displacement discontinuities. The separation phenomenon is analysed in the plasticity framework since an irreversible process occurs. The displacement discontinuity vector $\boldsymbol{w}$ is assumed to be the sum of a reversible (superscript e) and an irreversible (superscript p) contribution:

$$\dot{\boldsymbol{w}} = \dot{\boldsymbol{w}}^e + \dot{\boldsymbol{w}}^p \quad \text{and} \quad \dot{\boldsymbol{p}} = K_0\, \dot{\boldsymbol{w}}^e = K_0\, (\dot{\boldsymbol{w}} - \dot{\boldsymbol{w}}^p) \tag{1}$$

Damage initiation phase

According to the CMS model proposed in [1, 4], damage initiation occurs when the stress path achieves the piecewise linear *yield* or *activation function* shown in Fig. 1, where p_n is the normal traction, χ_0 its ultimate value in pure tension, p_t is the tangential traction, c_0 the cohesion and μ the Coulomb friction angle. The activation function consists of a vector of φ_y whose components or modes correspond to half-planes in the bi-dimensional stress space. The intersection of such half planes is a convex domain that constitutes the region of elastic behaviour of the joint. Each component φ_i depends on cohesive tractions $\boldsymbol{p}$ and static internal variables $\boldsymbol{\chi}$:

$$\varphi_i = \varphi_i(\boldsymbol{p}, \boldsymbol{\chi}) \begin{cases} < 0 & \text{inactive joint} \\ = 0 & \text{active joint} \end{cases}$$

The point where damage initiation occurs is called fictitious crack tip (shortened FCT). During the evolutionary process, it moves from the upstream edge to the downstream edge.

Damage evolution phase

Once the necessary activation condition $\varphi = 0$ is met, irreversible displacements $\dot{\boldsymbol{w}}^p$ can develop along the interface:

$$\dot{\boldsymbol{w}}^p = \frac{\partial Q(\boldsymbol{p}, \boldsymbol{\chi})}{\partial \boldsymbol{p}} \dot{\boldsymbol{\lambda}} \qquad \dot{\boldsymbol{\lambda}} \geq \mathbf{0} \tag{2}$$

where the *plastic potential* Q is defined in such a way that the interface fracture work without friction is controlled as explained later. The portion of joint where damage evolves is called fictitious process zone (shortened FPZ).

The main characteristic that differentiates the CMS model from Carol's [5] and Červenka's [6] is that all equations are linearised, hence the nonlinearity of the model is contained only in the complementarity conditions. A first set of five relations, also referred to as *Kuhn-Tucker conditions*, can be written with reference to the plastic multiplier $\dot{\lambda}_y$ associated with the inelastic displacement direction V_i (shown in Fig. 1):

$$\varphi_y \geq 0 \quad \dot{\lambda}_y \geq 0 \quad \varphi_y \dot{\lambda}_y = 0 \tag{3}$$

When the stress path is inside the elastic domain, all components φ_i are positive and therefore all components $\dot{\lambda}_i$ vanish. When the stress path achieves the activation function, a component φ_i vanishes and the corresponding $\dot{\lambda}_i$ becomes positive. A first set of complementarity relations specifies the conditions for the onset of softening along a branch.

Now a second set of complementarity relations has to be introduced. When the traction mode ($\varphi_1 = 0$) is activated, the linear softening law is completely determined by the condition that the energy dissipated is the traditional Mode I fracture energy $\mathcal{G}_F^I$ [7]. The softening branch is bounded; when the displacement discontinuity, along a pure traction mode, reaches the critical values $w_c = 2\,\mathcal{G}_F^I/\chi_0$, the cohesive forces vanish. The condition for the arrest of softening in this case can be written through a sixth complementarity relation.

Similarly, when two shear modes ($\varphi_4 = 0$) or ($\varphi_5 = 0$) are activated, the linear softening law is completely determined by the condition that the energy dissipated is the Mode II fracture energy $\mathcal{G}_F^{IIa}$ under high normal confinement and no dilatancy proposed by [8] in the context of the microplane model. The determination of pure Mode II fracture energy $\mathcal{G}_F^{II}$ would require a pure shear test, without normal confinement, which is extremely difficult to perform. That is the reason why $\mathcal{G}_F^{IIa}$ is preferred as a material property. The softening branch is bounded; when interface fracture work without contribution from friction, along a pure shear mode, reaches the critical value $\mathcal{G}_F^{IIa}$, the cohesive tractions vanish and the interaction forces are due to friction alone. The condition for the arrest of softening in this case can be written through a seventh complementarity relation. When the cohesive-frictional modes ($\varphi_2 = 0$ or $\varphi_3 = 0$) are activated, the critical condition is related to both displacement discontinuity components as shown in [1]. Along this separation mode,

when the condition for the arrest of softening is reached, the residual tangential stress is assumed as constant (see term $\bar{c}$ in Fig. 1).

The last complementarity relation of the model regards the dilatant behaviour associated with λ_2 and λ_3 (see μ_{d0} in Fig. 1). It appears reasonable to assume that there is a limit to the dilatancy of a joint. Therefore a plastic multiplier λ_8 is activated in order to store the total of λ_2 and λ_3 exceeding the parameter w_{dil}. Along this separation mode, when the condition for the arrest of softening is reached, the residual tangential stress is assumed to be dependent on Coulombian friction (see term $\mu|p_n|$ in Fig. 1).

MODELING WATER INSIDE THE CRACKS

As a consequence of additional damage occurring inside the FPZ due to the presence of water, it is assumed that fracture energy $\mathcal{G}_F$ reduces as pressure p_{w0} increases. The apparent value of $\mathcal{G}_F$ is assumed to be expressed by the following relationship [9]:

$$\hat{\mathcal{G}}_F = \mathcal{G}_F \left[1 - 2\,\frac{p_{w0}}{\chi_0} + \left(\frac{p_{w0}}{\chi_0}\right)^2\right] = \mathcal{G}_F\, S \tag{4}$$

The ratio $\frac{p_{w0}}{\chi_0}$ is identified as damage number. If $\frac{p_{w0}}{\chi_0} = 0$, i.e., $S = 1$, the material is considered undamaged and therefore, the softening law is derived from the traditional fracture energy measured in dry conditions. If $\frac{p_{w0}}{\chi_0} = 1$, i.e., $S = 0$, the material is considered fully damaged and fracture energy vanishes. The stress-opening law is now assumed in such a way that the openings are scaled through the factor S, i.e., $\hat{w} = S\,w$.

The pressure distribution is assumed to be described by two polynomial functions. Defining $\Psi = \frac{w}{w_{w0}}$ and $\Phi = \frac{p_w}{p_{w0}}$, we can write:

$$\Phi = f_1(\Psi) = a_1 + b_1\Psi + c_1\Psi^2 + d_1\Psi^3 \qquad \Psi \le \Psi_1 \tag{5}$$

$$\Phi = f_2(\Psi) = a_2 + b_2\Psi + c_2\Psi^2 + d_2\Psi^3 \qquad \Psi \ge \Psi_1 \tag{6}$$

It must be remarked that the eight constants of Eq. 6 are obtained by imposing six geometrical conditions and two mechanical conditions.

Value Ψ_0 corresponds to crack opening w below which $p_{w0} = 0$, while Ψ_1 corresponds to the knee point w_1. Values Ψ_0 and (Ψ_1, Φ_1) (transition point between f_1 and f_2) and value w_{w0} (shown in Fig. 2), are defined as ($\kappa \ge 2$ is a constant):

$$\Psi_0 = \Psi_1 - \frac{2}{\kappa}\,\Psi_1, \quad \Phi_1 = \frac{2\,\Psi_1}{2\Psi_1 + \kappa\,(1 - \Psi_1)}, \quad w_{w0} = \hat{w}_1 + \frac{2}{\xi}\,(\hat{w}_c - \hat{w}_1) \tag{7}$$

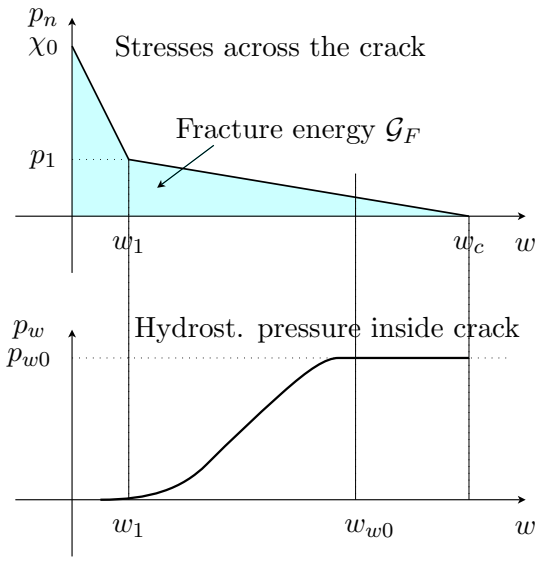

Figure 2. Water pressure distribution inside the crack.

Dam and found. Young modulus (Pa)	Dam and found. Poisson ratio –	χ_0 (Pa)	c_0 (Pa)	$\mathcal{G}_F^I$ (N/m)	$\mathcal{G}_F^{IIa}$ (N/m)	μ –	μ_{d0} –	w_1 (m)	w_c (m)
2.4e10	0.15	0.8e6	2.8e6	100	350	0.577	0.1	1.0e-4	4.5e-4

Table 1. Material properties.

EXAMPLE OF APPLICATION

As an example of application, the benchmark problem proposed in 1999 by the International Commission On Large Dams [3] was analysed (dam height 80m, base 60m). The gravity dam was discretized through 81081 elements, mainly quadrilateral with side of 0.16m. The foundation was subdivided into 15561 quadrilateral elements and the boundary into 555 infinite elements. Table 1 shows the material properties assumed. The parameter w_{dil} is taken to be 0.002m.

NUMERICAL RESULTS

The dam is analysed under self weight application, reservoir filling and imminent failure flood. Since the joint is the weakest part in the structure, the remaining material behaves in a linear elastic way.

Self weight application

In concrete dams, cracks are present and may be of considerable dimensions due to previous exceptional events [10]. Therefore, as a result of the damage experienced

by the dam in its history, an unbonded portion (0.8m) of the dam/foundation joint was assumed to pre-exist, starting from the upstream side.

During self weight application, this portion is closed and subjected to friction due to Poisson effect. In this phase no uplift pressure is applied. The corresponding crack mouth sliding displacement (CMSD) is opposite in sign with respect to the same displacement induced by water pressure during the reservoir filling phase. For the boundary condition analysed, since a high compressive field is applied at the tip of the unbonded joint zone, no damage growth occurs (all $\varphi_i < 0$ everywhere). This phase is modeled through the classical theory of elasticity and the theory of contact with Coulombian friction.

Reservoir filling

During the reservoir filling phase, as long as the joint is subjected to a high compressive field, the solution evolves following the elasto-friction regime previously described, with opposite sign of CMSD rate. The first damage occurs as soon as it becomes $\varphi_2 = 0$ or $\varphi_3 = 0$ at the less compressed edge of the joint. For the initial damage values analysed, this edge is always open when the full reservoir condition is reached.

Imminent failure flood

In this paper, the parameter controlling failure is the water level above the full reservoir condition, called overtopping water height (OVTH).

Figure 3 show crack opening displacement vs. the distance form upstream edge up to the peak value of OVTH. For the material properties and boundary conditions examined, the peak value of OVTH is found to be 2.5m.

Figure 4 show COD vs. OVTH diagram related to two points inside the FPZ. When OVTH grows from 0 to 0.17m, i.e. 2.1/1000 of dam height, COD grows from 0 to w_1.

CONCLUSIONS

For the material properties and boundary conditions analysed the following conclusions can be drawn:

- When FPZ is completely developed and the water penetrates inside the crack, a small cycle in water level (2.1/1000 of dam height) causes a complete unloading and reloading cycle in the FPZ.
- A reduction of $\mathcal{G}_F^I$ and $\mathcal{G}_F^{IIa}$, induced by a cyclic loading, has to be taken into account (see [11]).

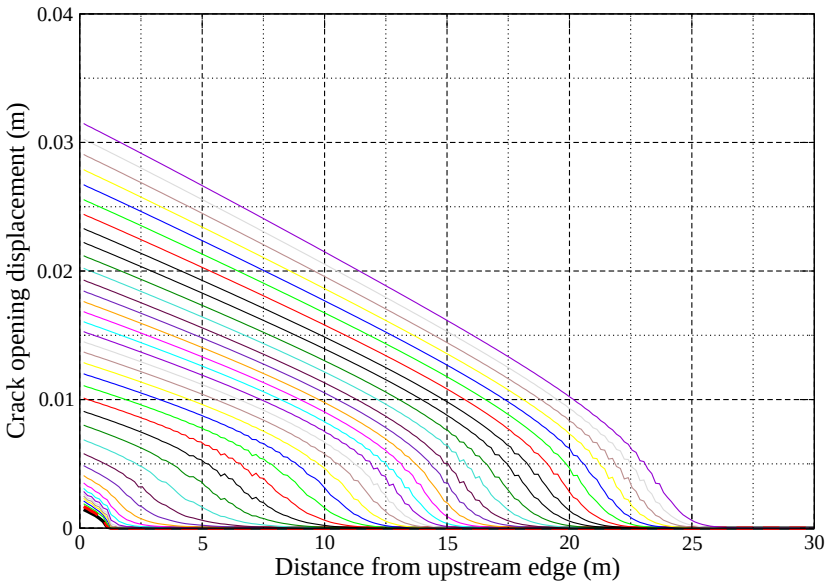

Figure 3. Crack opening displacement vs. distance from upstream edge.

ACKNOWLEDGMENTS

The financial support provided by the Italian Department of Education, University and Scientific Research (MIUR) to the research project on *"Diagnostic analyses and safety assessment of existing concrete dams"* (grant number 2004084599_004) is gratefully acknowledged.

REFERENCES

[1] Cocchetti, G., Maier, G. and Shen, X. (2002) Piecewise linear models for interfaces and mixed mode cohesive cracks. *Journal of Engineering Mechanics (ASCE)*, 3, 279–298.

[2] Reich, R., Brühwiler, E., Slowik, V. and Saouma, V., Experimental and computational aspects of a water/fracture interaction. In Bourdarot, E., Mazars, J. and Saouma, V., eds., *Dam Fracture and Damage*, 123–131. Balkema, Rotterdam (The Netherlands), 1994. ISBN 90 5410 369 8.

[3] ICOLD, Theme A2: Imminent failure flood for a concrete gravity dam. In *Fifth International Benchmark Workshop on Numerical Analysis of Dams*. Denver (CO), 1999.

[4] Bolzon, G. and Cocchetti, G. (2003) Direct assessment of structural resistance against pressurized fracture. *International Journal for Numerical and Analytical Methods in Geomechanics*, 27, 353–378.

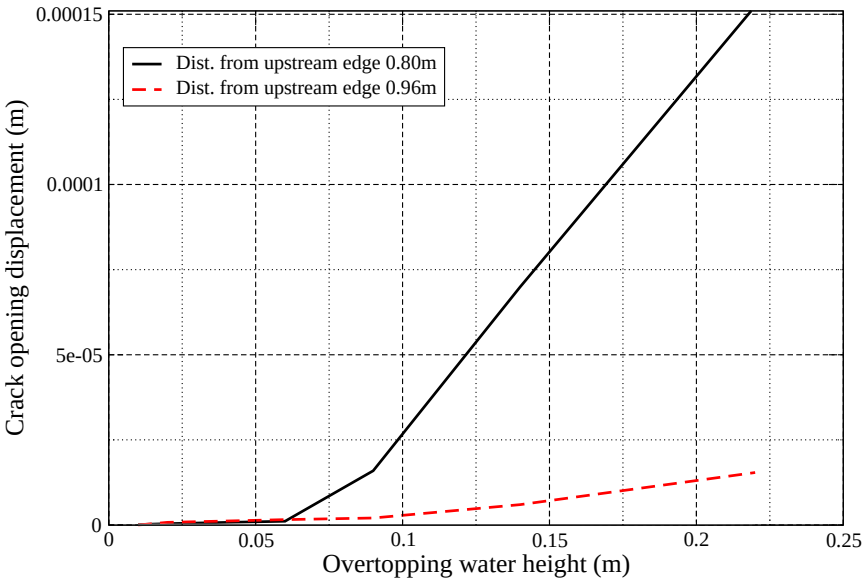

Figure 4. Examples of crack opening displacement vs. overtopping water height.

[5] Carol, I., Prat, P. and Lopez, C. (1997) A normal/shear cracking model: Application to discrete crack analysis. *Journal of Engineering Mechanics (ASCE)*, 123(8), 765–773.

[6] Červenka, J., Kishen, J. and Saouma, V. (1998) Mixed mode fracture of cementious bimaterial interfaces; part ii: Numerical simulations. *Engineering Fracture Mechanics*, 60(1), 95–107.

[7] Hillerborg, A., Modeer, M. and Petersson, P. (1976) Analysis of crack formation and crack growth in concrete by means of fracture mechanics and finite elements. *Cement and Concrete Research*, 6, 773–782.

[8] Carol, I., Bažant, Z. and Prat, P., Microplane-type constitutive models for distributed damage and localized cracking in concrete structures. In Bažant, Z., ed., *Fracture Mechanics of Concrete Structures*, 299–304. Elsevier Applied Science, The Netherlands, 1992.

[9] Reich, W., Brühwiler, E., Slowik, V. and Saouma, V., Experimental and computational aspects of a water/fracture interaction. 123–131. Balkema, The Netherlands, 1994.

[10] Rescher, O., Importance of cracking in concrete dams. In Rossmanith, H., ed., *Proceedings First International Conference on Fracture and Damage of Concrete and Rock*, 503–524. Pergamon Press, Oxford, 1990.

[11] Barpi, F. and Valente, S., Fatigue fracture in concrete structures. In 11^{th} *International Conference on Fracture, March 20-25, 2005 (Torino)*. 2005. Proceedings on CD-ROM.